Transient and Stability Analysis of Time-Domain Reactive Current Analyzers Using Averaged Waveforms

John Ofori-Tenkorang, *Student Member, IEEE*,
Jeff Chapman, *Student Member, IEEE,* and Bernard C. Lesieutre, *Member, IEEE*

Abstract— **A simple method of characterizing the transient response and the stability of time-domain analog reactive current analyzers is presented. The method of analysis, based on averaged waveforms, allows one to perform a linear analysis on an otherwise nonlinear system. The ability to predict the transient characteristics of these instrumentation circuits allows the instrumentation engineer to predict the settling time of the analyzer under various waveform measurement conditions and, more importantly, detect the presence of unstable equilibrium points in these nonlinear feedback circuits.**

I. Introduction

THE increased use of power electronic circuits in machine drives and industrial process control is causing substantial amounts of energy to be transmitted through nonsinusoidal voltages and currents. To reduce losses in the transmission network and achieve the maximum throughput of real power to the load, it is often necessary to design compensation circuits that minimize the amount of reactive current in the network. The power engineering community is split as to whether the problem of reactive current minimization under nonsinusoidal conditions should be tackled using a frequency-domain or time-domain approach. Frequency-domain methods provide insight on how the load impedance affects the flow of nonactive (or reactive) currents in the network; however, the design of an appropriate power-factor correction circuit requires that the susceptance of the load be known at all the harmonic frequencies present in the source voltage [1]. The time-domain approach, although sometimes obscure, does not require knowledge of the load impedance, and appropriate values for shunt reactance compensators for modest power factor correction,can be determined via analog instrumentation operating on the terminal voltages and currents [2]–[6].

The analog circuits suggested in [2]–[6], are nonlinear feedback circuits due to the presence of multipliers in the feedback loop. These circuits, to date, have only been analyzed in the steady state, and their transient performances which determine the choice of loop gains for reasonable settling times and also predict the stability of these circuits are yet to be characterized. The lack of such analysis has led to circuits such as the one proposed in [3], that are inherently unstable.

Manuscript received February 21, 1994; revised December 20, 1994.

The authors are with the Massachusetts Institute of Technology, Cambridge, MA 02139 USA.

Publisher Item Identifier S 0018-9456(96)00845-5.

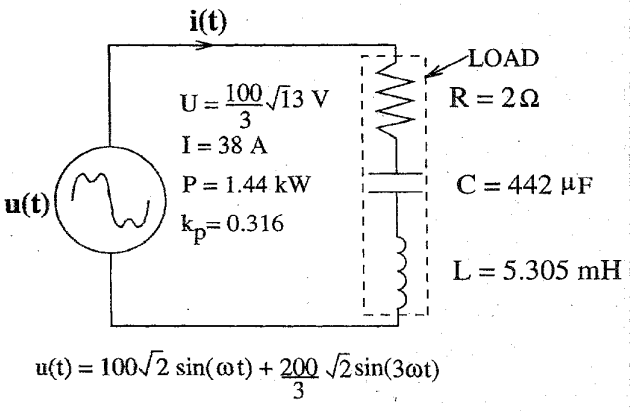

Fig. 1. LCR test circuit used in this paper.

In this paper, we present a simple method of analyzing the transient response and stability of these nonlinear feedback circuits that can aid designers to predict circuit performance and also assess the stability of novel circuit topologies for reactive current instrumentation. We note that the values of shunt capacitors and inductors obtained from the circuit topologies in [2]–[6] are only useful in networks with negligible source impedance, and hence in power systems with substantial inductive source impedance, these values of shunt reactors may be suboptimal [7]. However, this limitation does not detract from the method of analysis being presented here.

In this paper, we use a series LCR circuit fed by a nonsinusoidal voltage source, shown in Fig. 1, to illustrate the measurement of the equivalent load conductance G_e and hence the active or in-phase current, i_p, and power factor, k_p, in addition to the determination of optimum values of parallel shunt compensators for reactive current minimization or power factor correction. We start with power factor compensation via a single shunt capacitance C_{opt} as derived in [4], [9], followed by two-element shunt parallel LC compensation as suggested in [3].

II. Assumptions And Notation

In this paper, the source voltage $u(t)$ and source current $i(t)$ are assumed to be periodic with no dc component, and the source impedance of the supply voltage is assumed to be negligible. The time derivative of $u(t)$ and its integral

are denoted by $\dot{u}$ and $\breve{u}$, respectively. All rms quantities are denoted by uppercase.

Finally, we define the local average $\bar{\chi}(t)$ of an instantaneous variable $\chi(t)$ as

$$\bar{\chi}(t) \triangleq \frac{1}{T}\int_{t-T}^{t} \chi(\tau)\mathrm{d}\tau$$

such that the derivative of the time average is equal to the time average of the derivative of the instantaneous variable. That is,

$$\begin{aligned}\frac{d}{dt}\bar{\chi}(t) = \dot{\bar{\chi}}(t) &= \frac{1}{T}\int_{t-T}^{t}\frac{d}{dt}\chi(\tau)\mathrm{d}\tau \\ &= \frac{1}{T}\int_{t-T}^{t}\dot{\chi}(\tau)\mathrm{d}\tau \\ &= \bar{\dot{\chi}}(t)\end{aligned}$$

where T is the averaging interval. If $\bar{\chi}(t)$ is periodic with period T or any multiple thereof, we denote the averaged quantity as $\langle\chi\rangle$. Thus, we denote average values of all *periodic* quantities by angle brackets and local averages of *nonperiodic* quantities by overbars.

III. Measurement of Active Current and Load Power Factor

Consider the circuit shown in Fig. 1 where a linear load is powered by a nonsinusoidal voltage source $u(t) = \sqrt{2}\sum_n U_n \sin(n\omega_1 t)$. The admittance of the load at the nth harmonic frequency Y_{Ln} can be written as $Y_{Ln} = G_{Ln} + jB_{Ln}$. For the circuit of Fig. 1,

$$G_{Ln} = \frac{R(n\omega C)^2}{(n\omega RC)^2 + (n^2\omega^2 LC - 1)^2} \quad \text{and}$$

$$B_{Ln} = -\frac{jn\omega C(n^2\omega^2 LC - 1)}{(n\ megaRC)^2 + (n^2\omega^2 LC - 1)^2}.$$

The source current i consists of an active (in-phase) part, i_p, which is responsible for active power flow and a reactive or quadrature part i_q. The two components are mutually orthogonal such that the rms value of the source current, I, is given by $I = \sqrt{I_p^2 + I_q^2}$. In performing power factor correction, we seek to design compensation circuits that do not change i_p but minimize or eliminate i_q. The active current is given by

$$i_p(t) = \frac{P}{U^2}\cdot u(t) = G_e \cdot u(t)$$

where P is the active power delivered to the load, and G_e is the equivalent load conductance. Notice that i_p has the same shape as the supply voltage as shown in the last plot in Fig. 3. The load power factor k_p can be written in terms of frequency-domain quantities as

$$k_p = \frac{P}{UI} = \frac{\sum_n U_n I_n \cos(\phi_n)}{UI}$$

where ϕ_n is the phase angle between the voltage and the current at the nth harmonic, or in time-domain quantities as

$$k_p = \frac{P}{UI} = \frac{UI_p}{UI} = \frac{I_p}{I}.$$

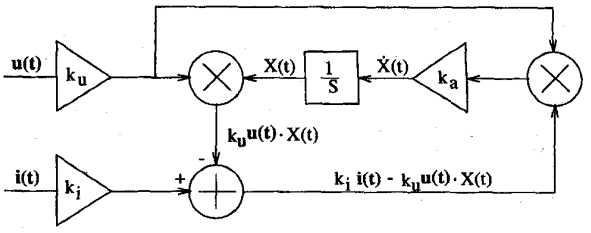

Fig. 2. Block diagram of circuit for measuring the equivalent load conductance, in-phase current, and quadrature current.

Notice that the frequency-domain approach requires the measurement of the rms values of all the harmonics in the voltage and current waveforms and the angle of the load impedance at all these frequencies, whereas the time-domain approach requires only the rms value of the active current to be measured.

A. Steady-State Equilibrium Points

A block diagram of a circuit that measures the active current (and hence active power) flowing into an arbitrary load from only the terminal voltage and current is shown in Fig. 2. This circuit corresponds to the first switch position of the Kusters and Moore circuit in [2, p. 1849]. It is easily shown that in the steady-state the average value of $X(t)$ is given by

$$\bar{X}_{ss} = \frac{k_i}{k_u}\cdot\frac{\langle u\cdot i\rangle}{\langle u\cdot u\rangle} = \frac{k_i}{k_u}\cdot\frac{P}{U^2} \tag{1}$$

where the ss subscript denotes the steady-state value [2], [3], [6]. Thus $\bar{X}_{ss}$ represents the equivalent load conductance G_e scaled by the ratio of the gains in the voltage and current attenuators. Equation (1) can be rewritten to isolate quantities of interest, namely the active power, P and the power factor, k_p, as

$$P = \frac{k_u}{k_i}\cdot\bar{X}_{ss}\cdot U^2 \quad \text{and} \quad k_p = \frac{P}{UI} = \frac{k_u}{k_i}\cdot\bar{X}_{ss}\cdot\frac{U}{I}. \tag{2}$$

BV. Transient Analysis

In order to determine the settling time of $\bar{X}(t)$ during instrumentation and, more importantly, the stability of the equilibrium point, we need to perform a transient analysis. The loop in Fig. 2 enforces that

$$\dot{X}(t) = k_a[k_i i - k_u u\cdot X(t)]k_u u \tag{3}$$

which leads to the nonlinear differential equation

$$\dot{X}(t) + k_a k_u^2[u\cdot u\cdot X(t)] = k_a k_u k_i[u\cdot i] \tag{4}$$

for the state variable X. To transform (4) into a constant coefficient linear differential equation, we employ the averaging procedure described in Section II and write (4) as

$$\bar{\dot{X}}(t) + \overline{k_a k_u^2[u\cdot u\cdot X(t)]} = \overline{k_a k_u k_i[u\cdot i]}. \tag{5}$$

If we assume that

1) $X(t)$ has small ripple such that over the averaging interval T, $X(t) \approx \bar{X}(t)$, and
2) $X(t)$ varies slowly so that $\bar{X}(t)$ does not vary significantly over the averaging interval T,

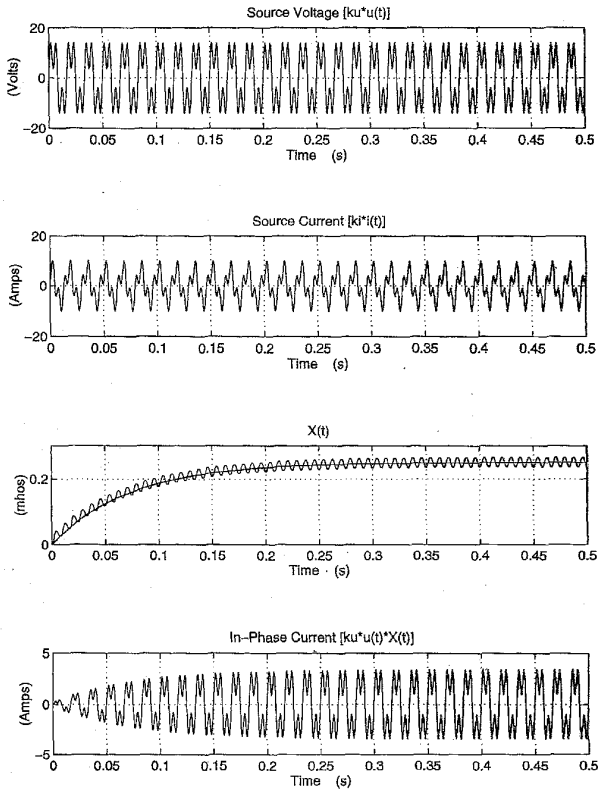

Fig. 3. Transient response of the system in Fig. 2.

then

$$\overline{k_a k_u^2 [u \cdot u \cdot X(t)]} \approx k_a k_u^2 \overline{u \cdot u} \bar{X}(t) \tag{6}$$

for constant $k_a k_u^2$ [8]. Using (6) with the knowledge that u and i are periodic, (5) becomes

$$\dot{\bar{X}}(t) + k_a k_u^2 \langle u \cdot u \rangle \bar{X}(t) = k_a k_u k_i \langle u \cdot i \rangle. \tag{7}$$

Therefore, the evolution of the local average, $\bar{X}(t)$, of the state variable $X(t)$ to a step in the input current (which corresponds to a step in the active power P under the condition of constant rms source voltage U) is given by

$$\begin{aligned} \bar{X}(t) &= \frac{k_i}{k_u} \cdot \frac{\langle u \cdot i \rangle}{\langle u \cdot u \rangle} \left(1 - e^{-t/\tau}\right) \\ &= \frac{k_i}{k_u} \cdot \frac{P}{U^2} \left(1 - e^{-t/\ au}\right) \end{aligned} \tag{8}$$

where the time constant $\tau = 1/k_a k_u^2 U^2$. Notice that the time constant τ is dependent on the size of the input, reflecting the nonlinear nature of the system.

To verify the above analysis, the system shown in Fig. 2 was simulated using SIMULINK™ on the LCR circuit in Fig. 1, where $U = (100/3) \cdot \sqrt{13}$ V and $P = 1444.44$ W.[1] For the waveforms shown in Fig. 3, the integrator gain k_a was set to 1, and the voltage and current attenuators k_u and k_i were set to 0.08 and 0.02, respectively, yielding a t me contant of 0.072 s. The steady-state value of $X(t)$ from Fig. 3 is 0.25. Superimposed on $X(t)$ is a plot of (8). This plot shows that the time constant nd steady-state values of the system in Fig. 2 are governed by (8)

$$P = \frac{k_u}{k_i} \cdot \bar{X}_{ss} \cdot U^2 = 1444.44\text{W}$$

$$k_p = \frac{k_u}{k_i} \cdot \bar{X}_{ss} \cdot \frac{U}{I} = 0.316$$

and the equivalent load conductance $G_e = k_u \bar{X}_{ss}/k_i = 0.1\mho$.

[1] In this simulation and subsequent ones, we have allowed significant ripple in the state va iables to accentuate their deviations from the computed local averages.

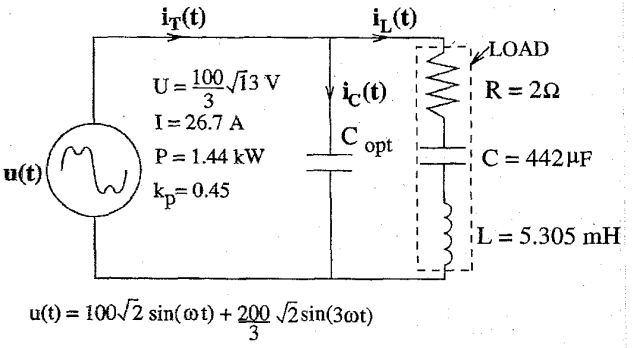

Fig. 4. Shunt capacitive compensation of circuit in Fig. 1.

IV. Capacitive Compensation with a Single Shunt Element

When we seek to improve the power factor of the load via connecting a shunt capacitor across the load, as shown in Fig. 4, the optimal capacitance C_{opt} has been shown using frequency-domain methods to be

$$C_{opt} = -\frac{\sum_n n U_n^2 B_n}{\omega \sum_n n^2 U_n^2}. \tag{9}$$

Here ω is the fundamental frequency, U_n is the rms value of the nth source voltage harmonic, and B_n is the load susceptance [5], [4], [9]. For the circuit of Fig. 4, C_{opt} as calculated by (9) is equal to 35.36 μF.

An equivalent expression for C_{opt} in terms of time-domain quantities can be derived as follows: if the connection of a shunt capacitance C across the load is to minimize the rms value of the total source current i_T, then we require that

$$\frac{d}{dC}\left(\frac{1}{T}\int_0^T i_T^2 \, \mathrm{dt}\right) = \frac{d}{dC}\left(\frac{1}{T}\int_0^T (i_C + i_L)^2 \, \mathrm{dt}\right) = 0 \tag{10}$$

where $i_C = C\dot{u}$. If the source impedance is zero, then the connection of C does not change the voltage, u, across the capacitor and the load. Thus the load current i_L is unchanged, and hence the derivative of u and i_L with respect to C are zero. Therefore, (10) can be written as

$$\begin{aligned} \frac{1}{T}\int_0^T 2\dot{u}(C\dot{u} + i_L) \, \mathrm{dt} = 0, \quad \Rightarrow \quad \frac{1}{T}\int_0^T \dot{u} \cdot i_L \, \mathrm{dt} \\ = -\frac{1}{T}\int_0^T C\dot{u}^2 \, \mathrm{dt}. \end{aligned}$$

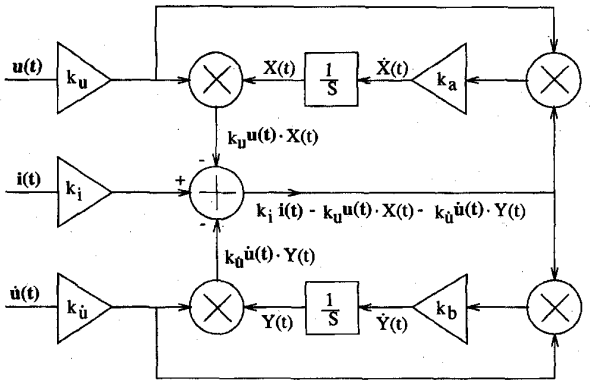

Fig. 5. Block diagram of circuit for determining G_e and C_{opt} simultaneously.

Thus

$$C = C_{opt} = -\frac{\frac{1}{T}\int_0^T \dot{u}\cdot i_L \,\mathrm{dt}}{\frac{1}{T}\int_0^T \dot{u}^2 \,\mathrm{dt}} = -\frac{\langle \dot{u}\cdot i\rangle}{\langle \dot{u}\cdot \dot{u}\rangle} \tag{11}$$

where we have replaced i_L with i; the original source current before the connection of the capacitor. It can be shown that (11) and (9) yield identical results [4].

Fig. 5 shows a block diagram of a circuit that determines the value of C_{opt} using time-domain waveforms. This block diagram corresponds to the second switch position presented in [2]. The top half measures the equivalent load conductance as in Fig. 2, while the bottom half determines C_{opt}. Variants of this circuit have been proposed in [3], [4], respectively, and in the steady state, it is easily shown that

$$\bar{X}_{ss} = \frac{k_i}{k_u}\cdot\frac{\langle u\cdot i\rangle}{\langle u\cdot u\rangle} \quad \text{and} \quad \bar{Y}_{ss} = \frac{k_i}{k_{\dot{u}}}\cdot\frac{\langle \dot{u}cdoti\rangle}{\langle \dot{u}\cdot \dot{u}\rangle}$$

which are just scaled versions of G_e and $-C_{opt}$, respectively.

A. Transient Analysis

The loops in Fig. 5 ensure that

$$\begin{aligned}\dot{X}(t) &= k_a[k_i i - k_u u\cdot X(t) - k_{\dot{u}}\dot{u}\cdot Y(t)]k_u u\\ &= k_a k_u k_i[u\cdot i] - k_a k_u^2[u\cdot u\cdot X(t)]\\ &\quad - k_a k_u k_{\dot{u}}[u\cdot \dot{u}\cdot Y(t)]\\ \dot{Y}(t) &= k_b[k_i i - k_u u\cdot X(t) - k_{\dot{u}}\dot{u}\cdot Y(t)]k_{\dot{u}}\dot{u}\\ &= k_b k_{\dot{u}} k_i[\dot{u}\cdot i] - k_b k_u k_{\dot{u}}[u\cdot \dot{u}\cdot X(t)]\\ &\quad - k_b k_{\dot{u}}^2[\dot{u}\cdot \dot{u}\cdot Y(t)].\end{aligned}$$

Making the "small ripple" and "slow variation" assumptions about the state variables $X(t)$ and $Y(t)$ and carrying out the averaging process, we obtain

$$\begin{aligned}\dot{\bar{X}}(t) &= -[k_a k_u^2\langle u\cdot u\rangle\bar{X}(t) + k_a k_u k_{\dot{u}}\langle u\cdot \dot{u}\rangle\bar{Y}(t)]\\ &\quad + k_a k_u k_i\langle u\cdot i\rangle\\ \dot{\bar{Y}}(t) &= -[k_b k_u k_{\dot{u}}\langle u\cdot \dot{u}\rangle\bar{X}(t) + k_b k_{\dot{u}}^2\langle \dot{u}\cdot \dot{u}\rangle\bar{Y}(t)]\\ &\quad + k_b k_{\dot{u}} k_i\langle \dot{u}\cdot i\rangle.\end{aligned}$$

These can be written in matrix form as

$$\begin{bmatrix}\dot{\bar{X}}(t)\\ \dot{\bar{Y}}(t)\end{bmatrix} = -\begin{bmatrix}k_a k_u^2\langle u\cdot u\rangle & k_a k_u k_{\dot{u}}\langle u\cdot \dot{u}\rangle\\ k_b k_u k_{\dot{u}}\langle u\cdot \dot{u}\rangle & k_b k_{\dot{u}}^2\langle \dot{u}\cdot \dot{u}\rangle\end{bmatrix}\begin{bmatrix}\bar{X}(t)\\ \bar{Y}(t)\end{bmatrix} + \begin{bmatrix}k_a k_u k_i\langle u\cdot i\rangle\\ k_b k_{\dot{u}} k_i\langle \dot{u}\cdot i\rangle\end{bmatrix} \tag{12}$$

where we have used the identity $\dot{\bar{X}}(t) = \dot{X}(t)$ and $\dot{\bar{Y}}(t) = \dot{Y}(t)$.

Since $\langle u\cdot \dot{u}\rangle = 0$, (12) simplifies to

$$\begin{bmatrix}\dot{\bar{X}}(t)\\ \dot{\bar{Y}}(t)\end{bmatrix} = -\begin{bmatrix}k_a k_u^2\langle u\cdot u\rangle & 0\\ 0 & k_b k_{\dot{u}}^2\langle \dot{u}\cdot \dot{u}\rangle\end{bmatrix}\begin{bmatrix}\bar{X}(t)\\ \bar{Y}(t)\end{bmatrix} + \begin{bmatrix}k_a k_u k_i\langle u\cdot i\rangle\\ k_b k_{\dot{u}} k_i\langle \dot{u}\cdot i\rangle\end{bmatrix} \tag{13}$$

showing that the differential equations for $\bar{X}(t)$ and $\bar{Y}(t)$ are decoupled, and the two halves of the circuit in Fig. 5 operate independently. Solving (13) gives

$$\bar{X}(t) = \frac{k_i}{k_u}\cdot\frac{\langle u\cdot i\rangle}{U^2}\left[1 - e^{-t/\tau_a}\right]$$

and

$$\bar{Y}(t) = \frac{k_i}{k_{\dot{u}}}\cdot\frac{\langle \dot{u}\cdot i\rangle}{\dot{U}^2}\left[1 - e^{-t/\tau_b}\right] \tag{14}$$

where $\tau_a = 1/k_a k_u^2 U^2$ and $\tau_b = 1/k_b k_{\dot{u}}^2 \dot{U}^2$. Inductive shunt compensation can also be achieved in a similar manner by replacing $\dot{u}$ with the integral $\breve{u}$ of the source voltage.

Once again, the time constants are inversely proportional to the size of the inputs. Therefore, in order to ensure that the circuit settles in a reasonable time when waveforms with small rms values are being analyzed, automatic gain controls (AGC's) may be needed to automatically adjust the amplitudes of $\dot{u}$ and $\breve{u}$. The AGC's are also needed if the circuit is to be used to analyze waveforms over a wide frequency range, since the outputs of the operational amplifiers used to compute $\breve{u}$ and $\dot{u}$ are proportional to the frequency of the input waveform.

Fig. 6 shows the transient response of the circuit in Fig. 5 for $k_u = 0.08$, $k_i = 0.2$, $k_{\dot{u}} = 9E-5$, $k_a = 0.15$, $k_b = 0.2$, $U = (100/3)\cdot\sqrt{13}$ V and $\dot{U} = 8.43E\mathrm{E}4$ V/s ; yielding $\tau_a = 0.072$ s and $\tau_b = 0.087$ s. The steady-state value of $\bar{X}(t)$ remains unchanged as in the previous simulation and that of $Y(t) = -0.0786$. Superimposed on the $X(t)$ and $Y(t)$ waveforms are their average values as predicted by

$$C_{opt} = -\frac{k_{\dot{u}}}{k_i}\cdot Y_{ss} = 35.36\,\mu\mathrm{F} \tag{15}$$

which is in agreement with (9). We note that the power factor with shunt capacitive compensation only increased slightly; from 0.32 to 0.45.

V. Parallel Two-Element Shunt Lc Compensation

It is possible to further improve the power factor of the circuit in Fig. 1 by using a parallel combination of a shunt capacitor and a shunt inductor, as shown in Fig. 7. Since the LC resonant frequency is between the two harmonics in the source voltage, it is possible to make the circuit resonant at

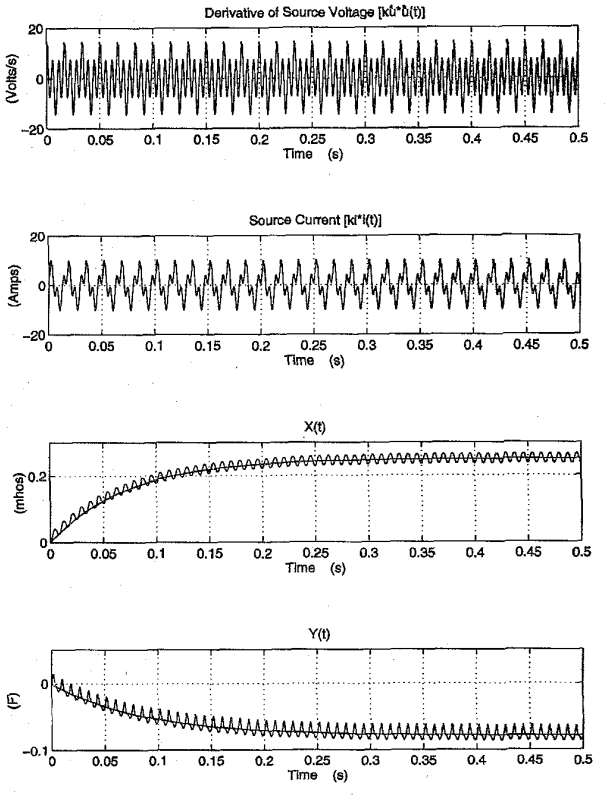

Fig. 6. Transient response of the system in Fig. 5.

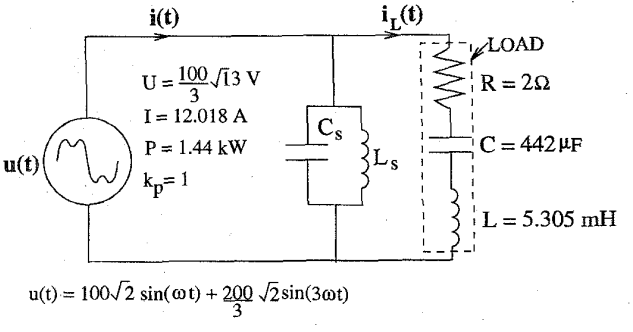

Fig. 7. Shunt LC compensation of the circuit in Fig. 1.

both harmonic frequencies. In the frequency domain the values of the appropriate shunt inductance L_s and shunt capacitance C_s can be found by solving two simultaneous equations that make the imaginary part of the combined shunt admittance of the load and compensator vanish at both harmonic frequencies. This analysis is straightfoward and will not be repeated here. The results from such analysis yield $L_s = 8.841$ mH and $C_s = 265.25$ μF.

It is shown in [3] that to minimize the rms value of the source current, L_s and C_s must satisfy the following two time-domain equations simultaneously:

$$\frac{\langle u \cdot u \rangle}{L_s} - C_s \cdot \langle \dot{u} \cdot \dot{u} \rangle = \langle \dot{u} \cdot i \rangle \tag{16}$$

$$C_s \cdot \langle u \cdot u \rangle - \frac{\langle \breve{u} \cdot \breve{u} \rangle}{L_s} == \langle \breve{u} \cdot i \rangle. \tag{17}$$

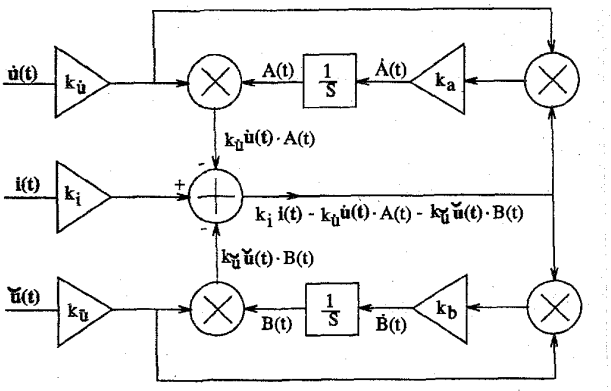

Fig. 8. Block diagram of circuit that solves (16) and (17).

Solving the preceding two equations yield,

$$L_s = \frac{\langle u \cdot u \rangle^2 - \langle \dot{u} \cdot \dot{u} \rangle \langle \breve{u} \cdot \breve{u} \rangle}{\langle u \cdot u \rangle \langle \dot{u} \cdot i \rangle + \langle \breve{u} \cdot i \rangle \langle \dot{u} \cdot \dot{u} \rangle} \tag{18}$$

and

$$C_s = \frac{\langle u \cdot u \rangle \langle \breve{u} \cdot i \rangle + \langle \breve{u} \cdot \breve{u} \rangle \langle \dot{u} \cdot i \rangle}{\langle u \cdot u \rangle^2 - \langle \dot{u} \cdot \dot{u} \rangle \langle \breve{u} \cdot \breve{u} \rangle}. \tag{19}$$

Note that (18) and (19) are written in terms of time-domain quantities obtainable from the source terminal voltage and current waveforms.

In [3], it was shown that the circuits with the block diagrams shown in Figs. 8 and 10 can be used to autmatically compute the values of C_s and L_s. Althouh both circuits have identical steady-state equilibrium points, a transient analysis shows that the circuit in Fig. 10 is unstable.

A. Transient Analysis

The loops in Fig. 8 ensure that

$$\begin{aligned}
\dot{A}(t) &= k_a[k_i i - k_{\dot{u}}\dot{u} \cdot A(t) - k_{\breve{u}}\breve{u} \cdot B(t)]k_{\dot{u}}\dot{u} \\
&= k_a k_{\dot{u}} k_i [\dot{u} \cdot i] \\
&\quad - k_a k_{\dot{u}}^2 [\dot{u} \cdot \dot{u} \cdot A(t)] - k_a k_{\dot{u}} k_{\breve{u}} [\dot{u} \cdot \breve{u} \cdot B(t)] \\
\dot{B}(t) &= k_b[k_i i - k_{\dot{u}}\dot{u} \cdot A(t) - k_{\breve{u}}\breve{u} \cdot B(t)]k_{\breve{u}}\breve{u} \\
&= k_b k_{\breve{u}} k_i [\breve{u} \cdot i] - k_b k_{\dot{u}} k_{\breve{u}} [\breve{u} \cdot \dot{u} \cdot A(t)] \\
&\quad - k_b k_{\breve{u}}^2 [\breve{u} \cdot \breve{u} \cdot B(t)]
\end{aligned}$$

which, after averaging, can be written in matrix form as

$$\begin{bmatrix} \dot{\bar{A}}(t) \\ \dot{\bar{B}}(t) \end{bmatrix} = -\begin{bmatrix} k_a k_{\dot{u}}^2 \langle \dot{u} \cdot \dot{u} \rangle & k_a k_{\dot{u}} k_{\breve{u}} \langle \dot{u} \cdot \breve{u} \rangle \\ k_b k_{\dot{u}} k_{\breve{u}} \langle \breve{u} \cdot \dot{u} \rangle & k_b k_{\breve{u}}^2 \langle \breve{u} \cdot \breve{u} \rangle \end{bmatrix} \begin{bmatrix} \bar{A}(t) \\ \bar{B}(t) \end{bmatrix} + \begin{bmatrix} k_a k_{\dot{u}} k_i \langle \dot{u} \cdot i \rangle \\ k_b k_{\breve{u}} k_i \langle \breve{u} \cdot i \rangle \end{bmatrix}. \tag{20}$$

Noting that $\langle \dot{u} \cdot \breve{u} \rangle = -U^2$ for periodic waveforms with no dc component, we can write (20) as

$$\begin{bmatrix} \dot{\bar{A}}(t) \\ \dot{\bar{B}}(t) \end{bmatrix} = \begin{bmatrix} -k_a k_{\dot{u}}^2 \langle \dot{u} \cdot \dot{u} \rangle & k_a k_{\dot{u}} k_{\breve{u}} U^2 \\ k_b k_{\dot{u}} k_{\breve{u}} U^2 & -k_b k_{\breve{u}}^2 \langle \breve{u} \cdot \breve{u} \rangle \end{bmatrix} \begin{bmatrix} \bar{A}(t) \\ \bar{B}(t) \end{bmatrix} + \begin{bmatrix} k_a k_{\dot{u}} k_i \langle \dot{u} \cdot i \rangle \\ k_b k_{\breve{u}} k_i \langle \breve{u} \cdot i \rangle \end{bmatrix} \tag{21}$$

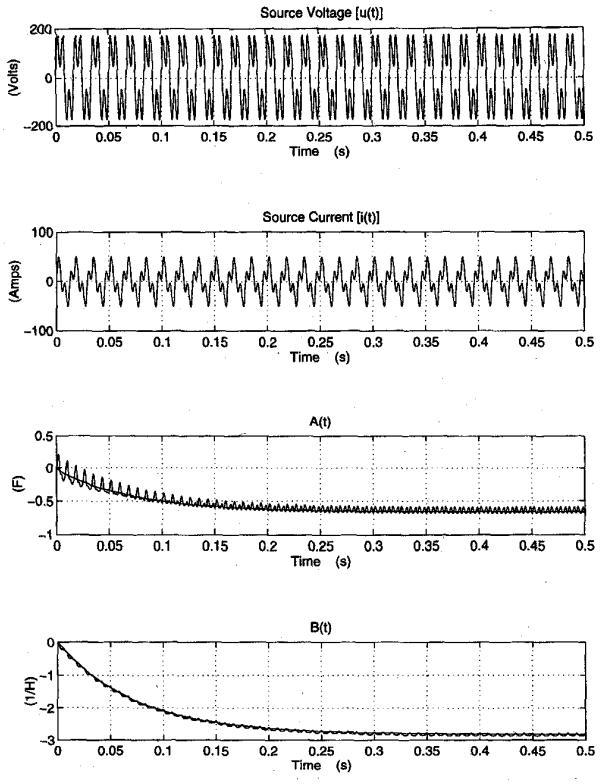

Fig. 9. Transient response of the system in Fig. 8.

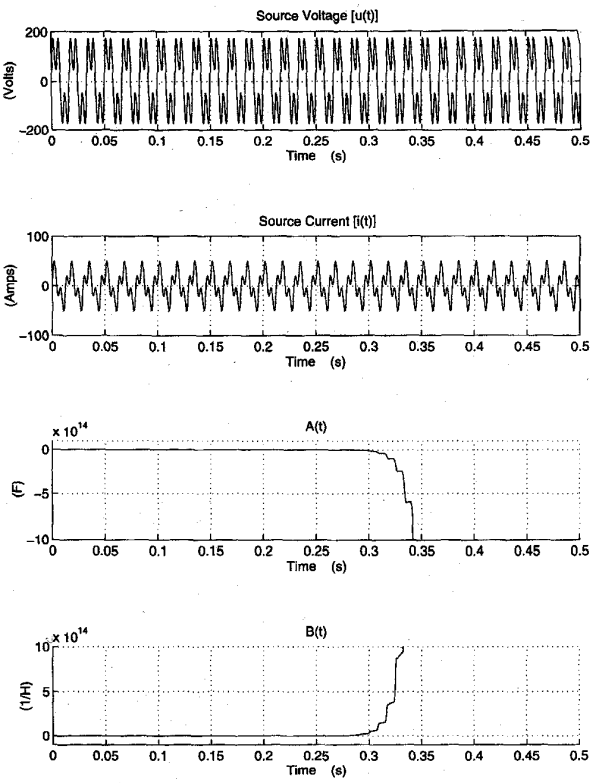

Fig. 11. Transient response of the system in Fig. 10.

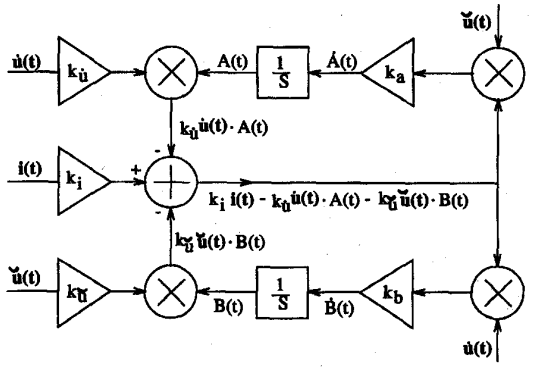

Fig. 10. Alternative circuit that solves (16) and (17).

$$= \begin{bmatrix} -a & b \\ c & -d \end{bmatrix} \begin{bmatrix} \bar{A}(t) \\ \bar{B}(t) \end{bmatrix} + \begin{bmatrix} k_a k_{\dot{u}} k_i \langle \dot{u} \cdot i \rangle \\ k_b k_{\dot{u}} k_i \langle \breve{u} \cdot i \rangle \end{bmatrix} \tag{22}$$

where a, b, c, and d are positive numbers. This system, unlike those in Section IV, is not decoupled. In the steady state, where $\dot{A}(t)$ and $\dot{B}(t)$ are zero, (21) and (22) yield

$$\bar{A}_{ss} = -\frac{k_i}{k_{\dot{u}}} \cdot \frac{\langle u \cdot u \rangle \langle \breve{u} \cdot i \rangle + \langle \dot{u} \cdot i \rangle \langle \breve{u} \cdot \breve{u} \rangle}{\langle u \cdot u \rangle^2 - \langle \dot{u} \cdot \dot{u} \rangle \langle \breve{u} \cdot \breve{u} \rangle} \tag{23}$$

and

$$\bar{B}_{ss} = -\frac{k_i}{k_{\breve{u}}} \cdot \frac{\langle u \cdot u \rangle \langle \dot{u} \cdot i \rangle + \langle \breve{u} \cdot i \rangle \langle \dot{u} \cdot \dot{u} \rangle}{\langle u \cdot u \rangle^2 - \langle \dot{u} \cdot \dot{u} \rangle \langle \breve{u} \cdot \breve{u} \rangle}. \tag{24}$$

Thus, from (18) and (19)

$$C_s = -\frac{k_{\dot{u}}}{k_i} \cdot \bar{A}_{ss} \quad \text{and} \quad L_s = -\frac{k_i}{k_{\breve{u}}} / \bar{B}_{ss}. \tag{25}$$

Using the Hurwitz criterion, we deduce that the system described by (22) is stable if $ad > bc$. That is

$$k_a k_{\dot{u}}^2 \dot{U}^2 \cdot k_b k_{\breve{u}}^2 \breve{u}^2 > k_a k_{\dot{u}} k_{\breve{u}} U^2 \cdot k_b k_{\dot{u}} k_{\breve{u}} U^2 \tag{26}$$

$$\Rightarrow \dot{U} \cdot \breve{U} > U \cdot U. \tag{27}$$

For a nonsinusoidal voltage u given by

$$u = \sum_n^N \sqrt{2} U_n \sin(n\omega t + \alpha_n)$$

it can be shown that

$$\frac{U}{\breve{U}} < \frac{\dot{U}}{U} \quad \Rightarrow \dot{U} \cdot \breve{U} > U \cdot U. \tag{28}$$

Thus, the inequality in (27) is always satisfied, and the system is always stable. Furthermore, for the condition given in (27), the eigenvalues of the syste matrix are never complex. Therefore the system response is never oscillatory for waveforms with constant $\langle \dot{u} \cdot i \rangle$ and $\langle \breve{u} \cdot i \rangle$.

Fig. 9 shows the simulated response of the circuit in Fig. 8 to a step input in power P for a nonsinusoidal input voltage. For this simulation, for $k_{\dot{u}} = 0.00008$, $k_i = 0.2$, $k_{\breve{u}} = 8$, $k_a = 4$, $k_b = 5$, $U = (100/3) \cdot \sqrt{13}$ V, $\dot{U} = 8.43E4$ V/s, and $\breve{U} = 0.2717$ V/s. The eigenvalues λ_1, λ_2 of the system

matrix are $\lambda_1 = -192.07$ and $\lambda_2 = -13.48$. The evolution of the average values of the state A and B is given by

$$\bar{A}(t) = A_{ss} + \left[C_1 e^{\lambda_1 t} + C_2 e^{\lambda_2 t}\right] \tag{29}$$

and

$$\bar{B}(t) = B_{ss} + \left[C_3 e^{\lambda_1 t} + C_4 e^{\lambda_2 t}\right], \tag{30}$$

where A_{ss} and B_{ss} are given by (23) and (24), respectively, and

$$C_1 = \frac{k_a k_{\dot{u}} k_i \langle \dot{u} \cdot i \rangle + \lambda_2 A_{ss}}{\lambda_1 - \lambda_2}$$

$$C_2 = \frac{k_a k_{\dot{u}} k_i \langle \dot{u} \cdot i \rangle + \lambda 1 A_{ss}}{\lambda_2 - \lambda_1}$$

$$C_3 = \frac{k_b k_{\breve{u}} k_i \langle \breve{u} \cdot i \rangle + \lambda_2 B_{ss}}{\lambda_1 - \lambda_2}$$

and

$$C_4 = \frac{k_b k_{\breve{u}} k_i \langle \breve{u} \cdot i \rangle + \lambda_1 B_{ss}}{\lambda_2 - \lambda_1}.$$

The plots of $\bar{A}(t)$ and $\bar{B}(t)$ are also superimposed on the simulation waveforms in Fig. 9. We see that the system is stable, and that the average values of the state variables evolve as predicted. Using the final values of $\bar{A}(t)$ and $\bar{B}(t)$ we calculate $C_s = 265.25$ μF and L_s as predicted. Using the final values of $\bar{A}(t)$ and $\bar{B}(t)$ we calculate $C_s = 265.25\mu$F and $L_s = 8.841$ mH from (25) by multiplication of A_{ss} and B_{ss} by the appropriate scaling factors.

With the values of shunt capacitance and inductance as calculated, the power factor of the circuit in Fig. 7 is now unity. In general, unity power factor may not be achieved unless the load conductance at all the harmonic frequencies is equal to the equivalent load conductance G_e [1], as is the case here.

In [3], it was also shown that the block diagram in Fig. 10 solved (16) and (17), and hence could be used to compute C_s and L_s. This circuit corresponds to Fig. 8 except that the inputs to the second multiplier, $\dot{u}$ and $\breve{u}$, are switched.

The differential equations for the averaged state variables are given by

$$\begin{bmatrix} \dot{\bar{A}}(t) \\ \dot{\bar{B}}(t) \end{bmatrix} = -\begin{bmatrix} k_a k_{\dot{u}} k_{\breve{u}} \langle \dot{u} \cdot \breve{u} \rangle & k_{\dot{u}^2} \langle \dot{u} \cdot \breve{u} \rangle \\ k_b k_{\dot{u}} k_{\breve{u}} \langle \dot{u} \cdot \dot{u} \rangle & k_b k_{\breve{u}} k_{\breve{u}} \langle \breve{u} \cdot \dot{u} \rangle \end{bmatrix} \begin{bmatrix} \bar{A}(t) \\ \bar{B}(t) \end{bmatrix} + \begin{bmatrix} k_a k_{\dot{u}} k_i \langle \dot{u} \cdot i \rangle \\ k_b k_{\breve{u}} k_i \langle \breve{u} \cdot i \rangle \end{bmatrix}. \tag{31}$$

Again, noting that $\langle \dot{u} \breve{u} \rangle = -U^2$ for periodic waveforms with no dc component, we can write (20) as

$$\begin{bmatrix} \dot{\bar{A}}(t) \\ \dot{\bar{B}}(t) \end{bmatrix} = \begin{bmatrix} k_a k_{\dot{u}} k_{\breve{u}} U^2 & -k_a k_{\dot{u}^2} \langle \dot{u} \cdot \dot{u} \\ -k_b k_{\breve{u}^2} \langle \breve{u} \cdot \breve{u} & k_b k_{\breve{u}}^2 k_{\breve{u}} U^2 \end{bmatrix} \begin{bmatrix} \bar{A}(t) \\ \bar{B}(t) \end{bmatrix} + \begin{bmatrix} k_a k_{\dot{u}} k_i \langle \dot{u} \cdot i \rangle \\ k_b k_{\breve{u}} k_i \langle \breve{u} \cdot i \rangle \end{bmatrix}. \tag{32}$$

For a stable system we require that

$$k_a k_{\dot{u}}^2 \dot{U}^2 \cdot k_b k_{\breve{u}}^2 \breve{U}^2 < k_a k_{\dot{u}} k_{\breve{u}} U^2 \cdot k_b k_{\dot{u}} k_{\breve{u}} U^2 \tag{33}$$

$$\Rightarrow \dot{U} \cdot \breve{U} < U \cdot U. \tag{34}$$

Equation (34) is the complement of (28); therefore this system is unstable as demonstrated by the step response in Fig. 11.

VI. Conclusion

Waveform averaging techniques can be used to transform the nonlinear models for the time-domain analog reactive current analyzers presented in [2]–[4] into linear differential equations with constant coefficients. Time-domain current analyzers provide useful information about the load, such as the active power supplied, reactive power and power factor, using only measurements of the terminal voltages and currents.

The waveform averaging technique presented here results in a linear model that is easily analyzed, allowing the circuit designer to predict the transient response and stability of the nonlinear feedback circuit. We have used this methodology in conjunction with an LCR load fed by a nonsinusoidal voltage, to analyze and confirm the transient behavior of time-domain current analyzers presented in [2]–[4], and in the process, have shown instability in one of the circuits presented in [3]. The technique employed here can also be used to characterize the transient behavior of the reactive current converter presented in [6] and other such nonlinear feedback circuits.

References

[1] L. S. Czarnecki, "Considerations on the reactive power in nonsinusoidal situation," *IEEE Trans. Instrum Meas.*, vol. IM-34, no. 3, pp. 399–404, Sept. 1985.

[2] N. L. Kusters and W. J. N. Moore, "On the definition of reactive power under nonsinusoidal conditions," *IEEE Trans. Power Appar. Syst.*, vol. PAS-99, no. 5, pp. 1845–1854, Sept./Oct. 1980.

[3] C. H. Page, "Reactive power in nonsinusoidal situation," *IEEE Trans. Instrum. Meas.*, vol. IM-29, no. 4, pp. 420–423, Dec. 1980.

[4] L. S. Czarnecki, "Converter of the optimal capacitance for nonsinusoidal system compensation to DC voltage," *Electron. Lett.*, vol. 17, no. 12, pp. 426–427, June 1981.

[5] ——, "Additional discussion to "Reactive power under nonsinusoidal conditions," *IEEE Trans. Power Appar. Syst.*, vol. PAS-102, no. 4, pp. 1023–1024, Apr. 1993.

[6] P. Filipski, "A new approach to reactive current and reactive power measurement in nonsinusoidal systems," *IEEE Trans. Instrum. Meas.*, vol. IM-29, no. 4, pp. 423–426, Dec. 1980.

[7] L. S. Czarnecki, "A time-domain approach to reactive current minimization in nonsinusoidal situations," *IEEE Trans. Instrum. Meas.*, vol. 39, no. 5, pp. 698–703, Oct. 1990.

[8] J. G. Kassakian, M. F. Schlecht, and G. C. Verghese, *Principles of Power Electronics*. Reading, MA: Addison-Wesley, 1991, pp. 270–271.

[9] W. Shepherd and P. Zand, *Energy Flow and Power Factor in Nonsinusoidal Circuits*. Cambridge: Cambridge Univ. Press, 1979.

John Ofori-Tenkorang (S'95) was born in Kwahu-Tafo, Ghana, on January 19, 1965. He received the S.B., S.M., and E.E. degrees in electrical engineering in 1989, 1992, and 1993, respectively, from the Massachusetts Institute of Technology, Cambridge. He is currently performing doctoral research on permanent magnet wheel motors and power electronics for electric vehicle propulsion at the Laboratory for Electromagnetic and Electronic Systems at MIT.

He is currently an Instructor-G at MIT. His professional interests include electromechanical devices and drives, power electronics and control, instrumentation electronics, analog circuit design, and microprocessor-based systems.

Mr. Ofori-Tenkorang holds one U.S. Patent and was the recipient of the 1995 MIT Carlton E. Tucker Teaching Award. He is a member of Tau Beta Pi, Eta Kappa Nu, and Sigma Xi.

Jeff Chapman (SM'89) received the B.S.E.E. degree from the University of California, Santa Barbara, in 1990 and the S.M. degree in electrical engineering with emphasis in power systems, from the Massachusetts Institute of Technology, Cambridge, in 1992. He is currently a Ph.D. student at MIT. His research interests include power systems control and nonlinear control.

Bernard C. Lesieutre (S'86–M'93) received the B.S., M.S., and Ph.D. degrees in electrical engineering from the University of Illinois, Urbana-Champaign, in 1986, 1988, and 1993, respectively.

He is currently an Assistant Professor, Department of Electrical Engineering, Massachusetts Institute of Technology, Cambridge. His research interests include machine modeling and power systems dynamics, stability and control.

Dr. Lesieutre is a member of Eta Kappa Nu.